Charge Transfer Dye in Various Polymers with Different Polarity: Synthesis, Photophysical Properties, and Unusual Aggregation-Induced Fluorescence Changes

Giseop Kwak,*,† Hyeryun Kim,† In-Kyu Kang,† and Sung-Hoon Kim‡

Department of Polymer Science, Kyungpook National University, 1370 Sankyuk-dong, Buk-ku, Daegu 702-701, Korea, and Department of Textile System Engineering, Kyungpook National University, 1370 Sankyuk-dong, Buk-ku, Daegu 702-701, Korea

Received November 11, 2008; Revised Manuscript Received January 1, 2009

ABSTRACT: A new pyran-based CTD monomer, allyl 2-(2,6-bis((*E*)-4-(dimethylamino)styryl)-4*H*-pyran-4-ylidene)-2-cyanoacetate (**2**), was successfully synthesized by Knoevenagel reaction. Copolymerization of **2** with styrene (St), methyl methacrylate (MMA), and acrylonitrile (AN) afforded copolymers with different polarity, P(St-*co*-**2**), P(MMA-*co*-**2**), and P(AN-*co*-**2**), respectively. IR and UV−vis absorption spectra revealed that **2** is incorporated into the copolymers. The **2** in the copolymers exhibited absorption and fluorescence properties which are completely different from **2**. All these copolymers showed significant blue shifts in emission relative to **2**. Also, their $\lambda_{\max,\mathrm{abs}}$ and $\lambda_{\max,\mathrm{em}}$ increased with an increase in dielectric constant (ε) of the polymer matrix in order PAN ($\varepsilon = 5.5$) > PMMA (3.3) > PSt (2.5). The copolymers in DMF showed blue shifts in emission along with aggregation by addition of methanol while copolymers in 1,4-dioxane showed a red shift. The fluorescence intensity of P(St-*co*-**2**) and P(MMA-*co*-**2**) decreased by aggregation while that of P(AN-*co*-**2**) increased.

Introduction

Charge transfer dyes (CTD) such as 4-(dicyanomethylene)-2-methyl-6-(*p*-(dimethylamino)styryl)-4*H*-pyran (DCM) have been intensively developed for applications used as photo- (PL) and electroluminescent (EL) materials in the fields of dye laser,[1] sensor,[2] dye-sensitized solar cell,[3] and OLED.[4] Their fluorescence properties are highly sensitive to changes in the external environment such as polarity and pH of media due to their intrinsic intramolecular charge transfer (ICT) character.[5] A variety of dye-incorporated polymers have been synthesized, and their advanced functions and applications such as fluorescence image patterning,[6] logic gate function,[7] sensors,[8] and organic light-emitting device (OLED) performances[9] were demonstrated. Incorporation of functional dyes into polymer matrices makes it possible to easily prepare films and thus to expend their applications to a solid state. Thus, fundamental studies on their syntheses and photophysical properties are still crucial for the exploration of new functions and applications in dye and polymer chemistry.

Meanwhile, when π-conjugating fluorophore molecules and polymers take a highly twisted structure in a dilute solution and also have a bulky substitutent, aggregation-driven nanoparticles can often induce a remarkably enhanced emission relative to the isolated molecules in an ideal solution.[10] According to some related recent papers, such an aggregation-induced enhanced emission (AIEE) is now believed to come from restricted intramolecular rotation as well as conformational planarization.[10f−h]

Aggregation can be regarded as a process changing from a solution to a solid. Thus, if a certain dye molecule was incorporated into a certain polymer chain, aggregation of the polymer would afford a new external environment to the dye molecules. Namely, the media surrounding the dye changes from solvent to polymer matrix, leading to a change in media polarity. As mentioned previously, the fluorescence properties of CTD are significantly dependent on media polarity. Thus, aggregation of CTD-incorporated polymer may influence the fluorescence color and intensity of CTD.

On the basis of this idea, we synthesized three different types of CTD-incorporated polymers by the copolymerization method and investigated their photophysical properties related to charge transfer character in solutions, solid films, and aggregates. Eventually, the fluorescence property of CTD within the polymers was significantly dependent on the polarity of the polymer matrix, and aggregation of the polymers resulted in a significantly different fluorescence changes of CTD in dependence of the polymer matrix polarity.

Experimental Section

Monomer Synthesis. *Allyl Cyano-2-(2,6-dimethyl-4H-pyran-4-ylidene)acetate.* A mixture of 2,6-dimethylpyran-4-pyrone (3 g, 24 mmol), allyl cyanoacetate, (3 g, 24 mol), and acetic acid (12.5 mL) was refluxed for 24 h. The crude solid obtained was filtered, washed with methanol, and recrystallized from methanol several times. Yield: 20%; mass (*m*/*z*) 231 (M^+). ^{1}H NMR (400 MHz, $CDCl_3$): δ 2.27 (s, 6H), 4.65 (d, 6H), 4.65 (d, 2H), 5.20 (d, 1H), 5.36 (d, 1H), 5.94 (m, 1H), 6.59 (s, 1H), 7.87 (s, 1H). EA: Anal. calcd for $C_{13}H_{13}NO_3$: C, 67.52; H, 5.67; N, 6.06. Found: C, 67.17; H, 5.72; N, 6.03%.

*Allyl 2-(2,6-Bis((E)-4-(dimethylamino)styryl)-4H-pyran-4-ylidene)-2-cyanoacetate (**2**).* A solution of allyl 2-cyano-2-(2,6-dimethyl-4*H*-pyran-4-ylidene)acetate (0.2 g, 0.9 mmol), 4-(dimethylamino)benzaldehyde (0.13 g, 1.8 mmol), and piperidine (0.09 mL) in 1-propane (20 mL) was refluxed for 24 h using a Dean−Stark trap. The reaction solution was cooled to room temperature, and the solid product was isolated and washed well with 1-propanol and dried. The crude product was recrystallized from methanol several times. Yield: 30%; mass (*m*/*z*) 493 (M^+). ^{1}H NMR (400 MHz, $CDCl_3$): δ 3.04 (s, 12H), 4.70 (d, 2H), 5.26 (d, 1H), 5.43 (d, 1H), 5.99 (m, 1H), 6.52 (d, 1H), 6.54 (d, 1H), 6.65 (s, 1H), 6.71 (d, 4H), 7.38 (s, 2H), 7.42 (s, 4H), 7.97 (s, 1H). EA: Anal. calcd for $C_{31}H_{31}N_3O_3$: C, 75.43; H, 6.33; N, 8.5. Found: C, 74.69; H, 6.41; N, 8.67%.

Synthesis of Polymers. *P(St-co-**2**) and P(MMA-co-**2**).* **2** (0.005 g, 0.01 mmol), styrene (St) (1 g, 9.60 mmol) or methyl methacrylate (MMA) (0.87 g, 9.60 mmol), and azobis(isobutyronitrile) (AIBN) (0.03 g, 0.19 mmol) were mixed under dry nitrogen. Then the flask

---

* Corresponding author: tel +82-53-950-7558; fax +82-53-950-6623; e-mail gkwak@knu.ac.kr.

† Department of Polymer Science.

‡ Department of Textile System Engineering.

10.1021/ma802532b CCC: $40.75

Scheme 1. Syntheses of a Pyran-Based Dye Monomer, 2, and Copolymers

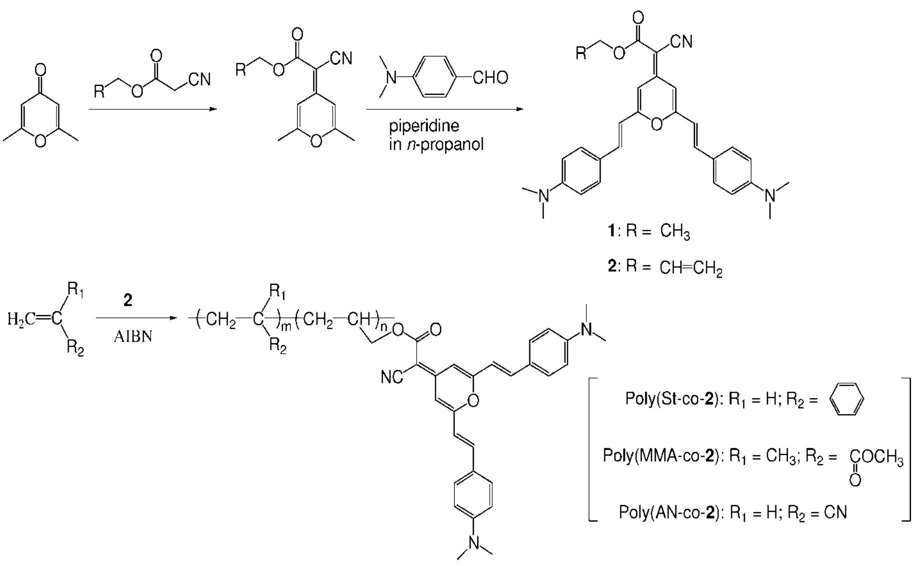

was immersed into an oil bath at 70 °C for 30 min. The crude products were dissolved in DMF and precipitated from methanol. To completely remove the unreacted **2** from the crude products, a Soxhlet extraction by water, methanol, and ethanol was conducted and was dried in a vacuum for 24 h.

*P(AN-co-***2***).* **2** (0.005 g 0.01 mmol), acrylonitrile (AN) (1 g, 17.8 mmol), azobis(isobutyronitrile) (AIBN) (0.03 g, 0.19 mmol) were dissolved in 10 mL of dry DMF under dry nitrogen. The solution was kept for 24 h at 70 °C. The polymerization mixture precipitated from methanol. To completely remove the unreacted **2**, a Soxhlet extraction by water, methanol, and ethanol was conducted and was dried in a vacuum for 24 h.

Measurements. The weight-average molecular weight (M_w) and number-average molecular weight (M_n) of P(St-*co*-**2**) and P(MMA-*co*-**2**) were evaluated using gel permeation chromatography (GPC, Alliance GPCV 2000). The intrinsic viscosity of P(AN-*co*-**2**) was obtained using a Ubbelohde viscometer. The UV−vis absorption spectra were measured on a JASCO V-650 spectrophotometer, and the photoluminescence spectra were recorded on a JASCO ETC-273 spectrofluorometer. The ^{1}H NMR spectra were measured in $CDCl_3$ containing tetramethylsilane as the internal standard using a Bruker Advance Digital 400 (400 MHz). The FT-IR spectra were recorded with a JASCO 620 spectrometer. The time-resolved emission spectra were measured on a streak camera using a femtosecond laser pulse from an optical parametric amplifier (Hamamatsu Photonics C4780). The center wavelength of 450 nm was used as the excitation light source. The width of the laser pulse was ~3 nm, and the repetition rate was 5 ns. These measurements were conducted at room temperature in air.

Results and Discussion

We already have reported the synthesis and fluorescence properties of a pyran-based CTD derivative, **1**, in a previous paper.[11] Its chemical structure is shown in Scheme 1. In order to incorporate such a dye molecule into a polymer chain, copolymerization of the dye with various vinyl monomers was thought as an appropriate method. Because **1** did not have any functional group for polymerization, however, **1** does not meet the purpose of this study. We thus designed a new CTD derivative, **2**, containing a polymerizable functional allyl group. As shown in Scheme 1, the synthetic method was very simple. The target monomer was easily obtained by two-step reactions including the Knoevenagel reaction. The ^{1}H NMR spectrum of **2** verified its well-defined chemical structure (Figure S1 in Supporting Information). Characteristic peak signals due to the allyl group appeared around 5.26, 5.43, and 5.99 ppm.

Table 1. Copolymerization of 2 with Various Vinyl Comonomers of St, MMA, and AN

run	**2** in feed mol%	copolymer					
		name	yeild wt%[c]	**2** unit mol%[d]	$M_w/10^3$ [e]	M_w/M_n [e]	feature
1[a]	0.10	P(St-co-**2**)	81	0.09	49.7	3.51	
2[a]	0.10	P(MMA-co-**2**)	95	0.07	130	2.39	
3[b]	0.06	P(AN-co-**2**)	68	0.05	-[f]	-	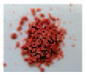

[a] Polymerized in bulk with AIBN as initiator at 70 °C for 30 min. [b] Polymerized in DMF with AIBN as initiator at 70 °C for 24 h. [c] To completely remove unreacted **2**, Soxhlet extraction by water, methanol, and ethanol was conducted in turn until the extracts do not show absorption due to **2** in a visible region. [d] Measured by UV−vis absorption analysis. [e] Measured in THF by GPC. [f] This polymer was insoluble in THF. Intrinsic viscosity was alternatively measured in DMF at 25 °C with a Ubbelohde viscometer to be estimated to 0.51.

Table 1 describes the copolymerization results of **2** with various vinyl monomers of styrene (St), methyl methacrylate (MMA), and acrylonitrile (AN). A large composition of **2** within the polymer chain may result in a fluorescence self-quenching even in a solution. To avoid that, an extremely small amount of 0.10−0.06 mol % **2** was used in copolymerization. Polymers from the copolymerizations of **2** with St, MMA, and AN were named as P(St-*co*-**2**), P(MMA-*co*-**2**), and P(AN-*co*-**2**), respectively. These polymers were obtained in high yields of 68−95%. P(St-*co*-**2**), P(MMA-*co*-**2**), and P(AN-*co*-**2**) appeared in yellow, orange, and red powders, respectively. The weight-average molecular weights (M_w) of P(St-*co*-**2**) and P(MMA-*co*-**2**) in THF were estimated to be 4.97 × 10^4 (M_w/M_n = 3.51) and 1.30 × 10^5 (2.39), respectively. Because P(AN-*co*-**2**) did not dissolve in THF, its viscosity was alternately measured to be calculated to 0.51. P(St-*co*-**2**) and P(MMA-*co*-**2**) dissolved well in DMF, methylene chloride, dichloroethane, THF, chloroform, toluene, and 1,4-dioxane, whereas P(AN-*co*-**2**) dissolved exclusively in a polar solvent of DMF. This hints that P(AN-*co*-**2**) is more polar than the other copolymers.

To know the composition of **2** within the copolymers, we first calculated the molar absorptivity (ε_{abs}) of **2** from the

Table 2. Absorption and Emission Properties of 2 and Copolymers in Various Solutions and Films

	$\lambda_{max,abs}$, nm	$\lambda_{max,em}$, nm	fwhm, nm									
	monomer			copolymer								
solution (ε)	**2**			P(St-*co*-**2**)			P(MMA-*co*-**2**)			P(AN-*co*-**2**)		
dioxane (2.22)	462	564	56.8	451	546	63.0	462	567	60.7	—[a]	—[a]	—[a]
toluene (2.38)	467	556	77.0	453	528	67.3	467	561	57.2	—[a]	—[a]	—[a]
chloroform (4.81)	479	585	66.6	464	556	70.1	476	582	68.4	—[a]	—[a]	—[a]
THF (7.52)	470	595	77.5	457	560	57.2	469	593	82.0	—[a]	—[a]	—[a]
methylene chloride (8.93)	481	601	75.1	461	561	55.6	477	603	78.7	—[a]	—[a]	—[a]
dichloroethane (10.42)	482	614	51.6	463	563	57.7	479	603	82.5	—[a]	—[a]	—[a]
acetonitrile (36.64)	476	624	94.4	—[a]	—[a]	—[a]	471	591	79.2	—[a]	—[a]	—[a]
DMF (38.25)	486	616	95.3	472	585	74.1	475	597	86.8	476	599	83.8
film	497[b]	637[b]	70.8[b]	457[c]	543[c]	71.2[c]	473[c]	561[c]	58.9[c]	476[c]	580[c]	85.9[c]

[a] Insoluble. [b] The film was made by thermal evaporation. [c] The film was made by the solvent-casting method.

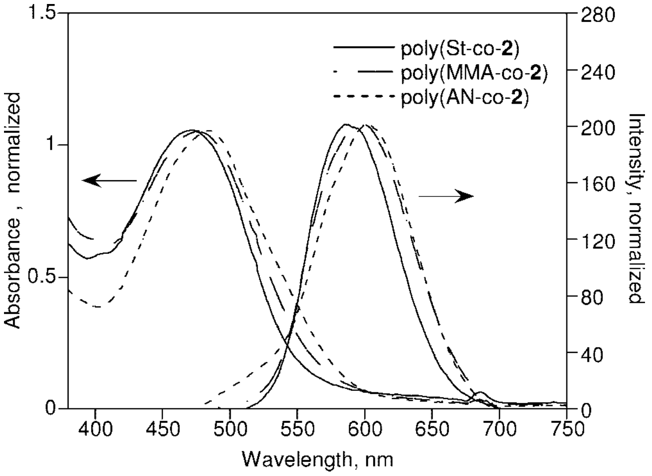

Figure 1. UV−vis absorption and fluorescence spectra of copolymers in DMF ($c < 1.0 \times 10^{-7}$ M).

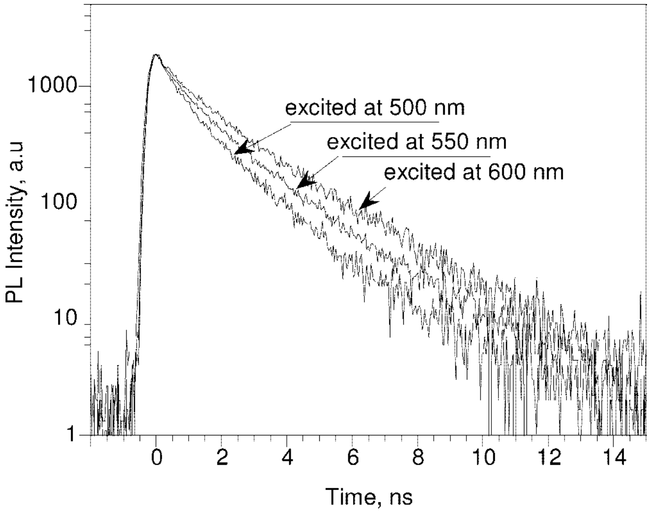

Figure 2. Time-resolved emission decay curve of P(St-*co*-**2**) in cast film at three different emission wavelengths.

calibration curve of absorbance at 485 nm in a concentration range of 3.80×10^{-6}−1.14×10^{-5} (Figure S2 in Supporting Information). The ε_{abs} value of **2** was considerably great as 2.46×10^5 L mol^{-1} cm^{-1}. Based on Beer−Lambert law of $A = \varepsilon_{abs}CL$, where A is absorbance, C is a mole concentration, and L is cell length, the mole fractions of **2** to St, MMA, and AN were calculated to be approximately 0.09, 0.07, and 0.05, respectively, as described in Table 1. These are slightly lower than the feed mole ratios. This is probably due to the less reactive allyl group of **2** relative to vinyl group of comonomers.

Owing to the small composition of the dye within the copolymers, ^{1}H NMR spectroscopy measurement was not preferable to verify the presence of dye incorporated into the copolymers. On the other hand, the IR spectra of the copolymers clearly verified the presence of dye in the copolymer chains by appearances of absorption peaks around 2300 and 1700 cm^{-1} due to C≡N stretching and C═O stretching motions, respectively (Figure S3 in Supporting Information).

Table 2 describes UV−vis absorption and emission properties of **2**, P(St-*co*-**2**), P(MMA-*co*-**2**), and P(AN-*co*-**2**) in various solvents with different polarity. Their absorption maximum wavelengths ($\lambda_{max,abs}$) shifted to longer wavelengths with an increase in the dielectric constant of solvent. Such a red shift along with dielectric constant was more significantly shown in fluorescence spectra. Large solvatochromism was observed in PL emission spectra of all copolymers as well as **2**. The fluorescence band significantly shifted to a longer wavelength with an increase in the dielectric constant of the solvent. For example, the emission maximum ($\lambda_{max,em}$) of P(St-*co*-**2**) varied from 546 nm (fwhm = 63.0 nm) in nonpolar dioxane to 585 nm (fwhm = 74.1 nm) in polar DMF. Similarly, large effects were observed in the PL emission of other copolymers as well as **2**. The much larger solvatochromic shifts in the PL emission spectra relative to those in the absorption spectra suggest that these compounds are highly polar in excited states rather than in ground states. Also, the full width at half-maximum (fwhm) of the polymers increased dramatically with solvent polarity. This indicates that the dye has more complex, plural excited species in a polar solution rather than in a nonpolar solution.

Table 3. Fluorescence Lifetimes of Copolymers in Films[a]

copolymer	monitor wavelength, nm	in cast film		
		τ_1 (f_1), ns	τ_2 (f_2), ns	χ^2
P(St-*co*-**2**)	500	0.63 (0.66)	1.91 (0.34)	2.08
	550	0.96 (0.67)	2.47 (0.33)	1.62
	600	1.10 (0.54)	2.64 (0.46)	1.37
P(MMA-*co*-**2**)	525	0.93 (0.33)	2.44 (0.67)	1.68
	575	1.12 (0.27)	2.76 (0.72)	1.33
	625	0.96 (0.10)	2.91 (0.90)	1.64
P(AN-*co*-**2**)	550	0.53 (0.66)	2.08 (0.34)	2.78
	600	0.73 (0.56)	2.30 (0.44)	2.37
	650	0.84 (0.44)	2.49 (0.56)	1.46

[a] τ_1 and τ_2 are lifetimes (ns), f_1 and f_2 are fractional intensities, and χ^2 is the reduced chi-square.

Figure 1 shows the UV−vis absorption and fluorescence spectra of the present copolymers in a polar DMF. P(St-*co*-**2**), P(MMA-*co*-**2**), and P(AN-*co*-**2**) showed $\lambda_{max,em}$ at 585, 597, and 599 nm, respectively, indicating a red shift along with an increase in the dielectric constant (ε) of the polymer matrix as expected from the order PAN (5.5) > PMMA (3.3) > PSt (2.5).[12] This indicates that the polymer matrix polarity significantly influences the ICT character of the dye molecule even in a solution state. On the other hand, their $\lambda_{max,abs}$ of P(St-*co*-**2**), P(MMA-*co*-**2**), and P(AN-*co*-**2**) in a same solvent of DMF are

Table 4. Photographs of 2, P(St-*co*-2), P(MMA-*co*-2), and P(AN-*co*-2) in Various Solutions and Films[a]

	Materials	Solutions								Film
		dioxane (ε=2.22)	toluene (2.38)	$CHCl_3$ (4.81)	THF (7.52)	methylene chloride (8.93)	dichloro-ethane (10.42)	acetonitrile (36.64)	DMF (38.25)	
Monomer	**2**									
Copolymer	P(St-co-**2**)							-[b]		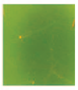
	P(MMA-co-**2**)									
	P(AN-co-**2**)	-[b]	-[b]	-[b]	-[b]	-[b]	-[b]	-[b]		

[a] Excited at >450 nm. [b] Insoluble.

Table 5. Comparison of the UV−vis Absorption Maxima Wavelengths ($\lambda_{max,abs}$) and Fluorescence Maxima Wavelengths ($\lambda_{max,em}$) of the Copolymers and 2-Dispersed Polymers in DMF

	monomer	copolymers			**2**-dispersed polymers		
	2	P(St-*co*-**2**)	P(MMA-*co*-**2**)	P(AN-*co*-**2**)	**2**-dispersed PSt	**2**-dispersed PMMA	**2**-dispersed PAN
$\lambda_{max,abs}$	486	472	475	476	485	485	485
$\lambda_{max,em}$	616	585	597	599	622	624	622

almost indentical. Moreover, the polymer matrix polarity effect was clearer in film as described in Table 2. The $\lambda_{max,em}$ of P(St-*co*-**2**), P(MMA-*co*-**2**), and P(AN-*co*-**2**) in films were 543, 561, and 580 nm, respectively.

The CTDs are able to vary their conformation and the effective conjugating sequence length due to a molecular rotation. Accordingly, their electronic states are often widely distributed, leading to the production of plural photoexcited emission species. Although their photoemission decays may obey multiexponential decay due to the distributions, a time course decay curve analysis using the multiexponential decay functions may help us to understand the excited-state dynamics semiquantitatively. In order to investigate the dynamic fluorescence properties of the present copolymers, we measured their fluorescence lifetimes with time-resolved fluorescence spectroscopy. For example, Figure 2 shows the time-resolved emission decay curve of P(St-*co*-**2**). Table 3 summarizes the fluorescence lifetimes of P(St-*co*-**2**), P(MMA-*co*-**2**), and P(AN-*co*-**2**) in films. Two exponentials are required to adequately fit the observed decay dynamics. The emissions of P(MMA-*co*-**2**) are characterized by a longer dominant fluorescence lifetime (τ_2) rather than a shorter one (τ_1). Longer emission wavelengths correlated with the longer lifetimes. The dominant lifetimes, τ_2, of P(MMA-*co*-**2**) at 525, 575, and 625 nm were 2.44, 2.76, and 2.91 ns, respectively, reflecting a fluorescence relaxation time for energy migration from higher to lower energy levels. In contrast with P(MMA-*co*-**2**), the emissions of P(St-*co*-**2**) and P(AN-*co*-**2**) are characterized by a shorter dominant fluorescence lifetime (τ_1) rather than a longer one (τ_2). For example, the dominant lifetimes, τ_1, of P(St-*co*-**2**) at 500, 550, and 600 nm were 0.63, 0.96, and 1.10 ns, respectively. These results indicate that the fluorescence relaxation of **2** is slower in P(MMA-*co*-**2**) than in other polymers. This may be explained by the idea that exciton deconfinement along with molecular rotational motion, and intramolecular exciton migration, are differently restrained according to the side-chain bulkiness as well as the polymer polarity.

Table 4 shows the actual photographs of the fluorescence colors of **2**, P(St-*co*-**2**), P(MMA-*co*-**2**), and P(AN-*co*-**2**) in various solutions and film. The fluorescence colors are completely different from each other. The difference in emission color is clearly recognized by the naked eyes. For example, P(St-*co*-**2**) in dioxane, P(St-*co*-**2**) in THF, P(MMA-*co*-**2**) in $CHCl_3$, P(St-*co*-**2**) in DMF, and **2** in acetonitrile appeared in green, yellow, orange, pink, and red, respectively.

The optical properties of the present copolymers in a polar DMF were compared with the corresponding **2**-dispersed polymers as summarized in Table 5. The dye monomer, **2**, shows $\lambda_{max,abs}$ and $\lambda_{max,em}$ at 486 and 616 nm, respectively. The copolymers show blue shifts in emission relative to **2**, while the **2**-dispersed polymers show almost the same $\lambda_{max,abs}$ and $\lambda_{max,em}$ as **2**. For example, P(St-*co*-**2**) shows $\lambda_{max,abs}$ and $\lambda_{max,em}$ at 472 and 585 nm, respectively, whereas the **2**-dispersed PSt absorbed at 485 nm in maximum and emitted at 622 nm in maximum. This indicates that the CTD molecule incorporated into the polymer chain is significantly influenced by the polymer matrix polarity as well as solvent polarity even at the isolated state in a dilute solution.

In such CTD-incorporated polymer systems, aggregation may more significantly influence the environment around the dye. We thus examined the aggregation effect on fluorescence by addition of a poor solvent of methanol to the DMF solutions of the copolymers. The DMF/methanol mixtures were vigorously stirred to ensure uniform dispersion of the polymer aggregates. The resultant solutions were macroscopically homogeneous and visually clear with no precipitate. Figure 3 exhibits the variation of emission spectra of the present copolymers by addition of methanol. All copolymers showed significant blue shifts in emission along with aggregation. For example, the emission band of P(St-*co*-**2**) shifted to a shorter wavelength by about 20 nm with addition of 40 vol % of methanol as shown in Figure 3a. Namely, with an increase in degree of aggregation, the dye molecule incorporated into the polymer chain becomes surrounded by the nonpolar polymer of PSt ($\varepsilon = 2.5$)[13] instead of

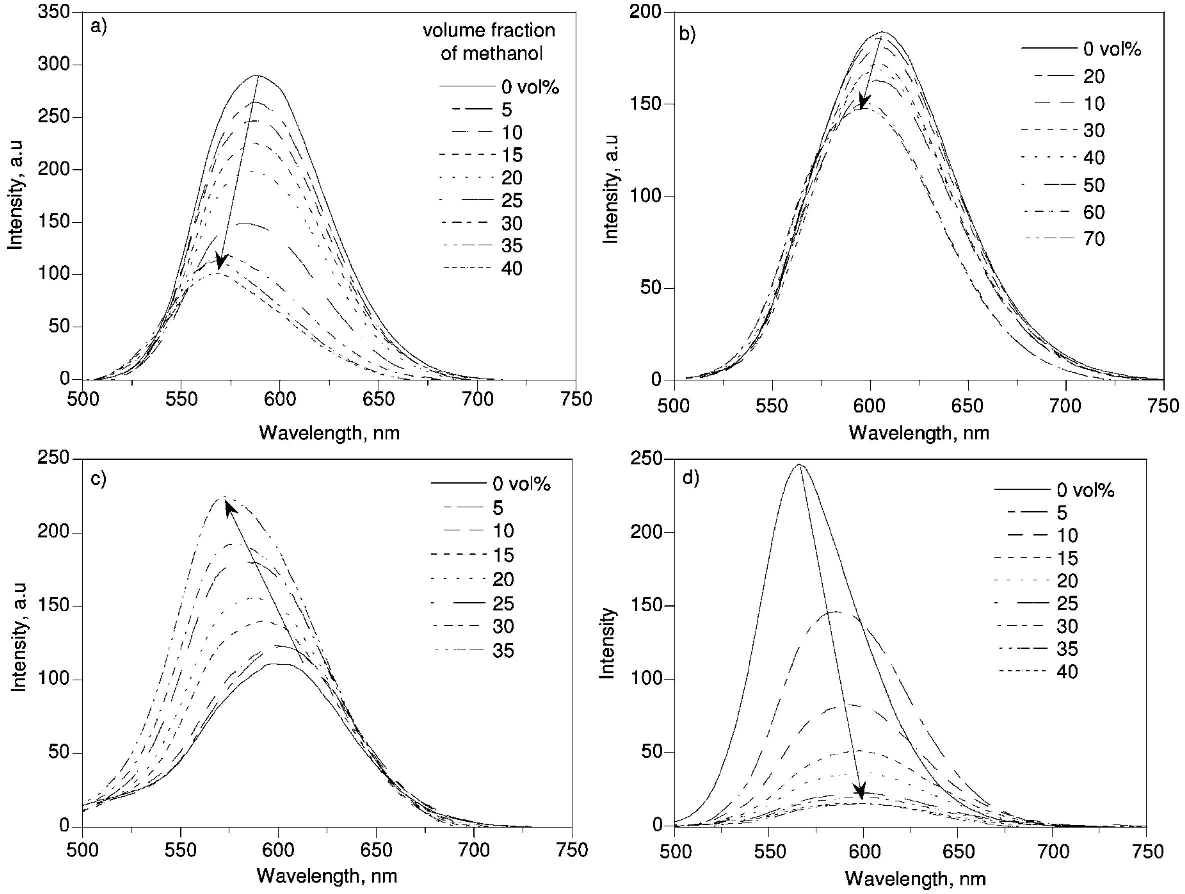

Figure 3. Variation in fluorescence spectra of (a) P(St-*co*-**2**), (b) P(MMA-*co*-**2**), and (c) P(AN-*co*-**2**) in DMF and (d) P(MMA-*co*-**2**) in dioxane ($c < 1.0 \times 10^{-7}$ mol L^{-1}) by addition of methanol.

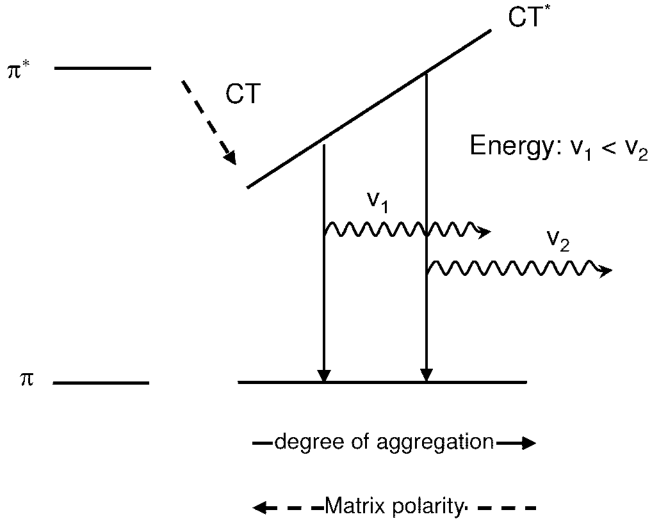

Figure 4. A proposed transition energy diagram of P(St-*co*-**2**) in DMF along with aggregation. CT denotes charge transfer transitions.

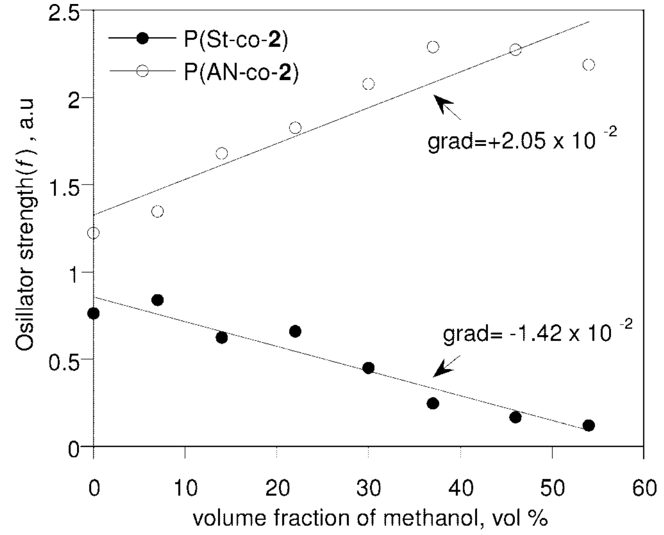

Figure 5. Plots of oscillator strength (*f*) of P(St-*co*-**2**) and P(AN-*co*-**2**) as functions of methanol fractions.

the polar solvent of DMF ($\varepsilon = 38.25$).[12] As proposed by the transition energy diagram shown in Figure 4, the aggregation of polymer reduces the polarity of environment surrounding dye, and thus, the energy of the CT excited state will increase, leading to a shorter wavelength light emission. On the other hand, the **2** hardly showed changes in $\lambda_{\mathrm{max,abs}}$ and $\lambda_{\mathrm{max,em}}$ although the emission intensity slightly decreased. All the **2**-dispersed polymers showed also no changes in $\lambda_{\mathrm{max,abs}}$ and $\lambda_{\mathrm{max,em}}$. In contrast to the cases of aggregations of copolymers in a polar solvent, the copolymers in a nonpolar solvent showed red shifts in emission along with aggregation. For example, as shown in Figure 3d, P(MMA-*co*-**2**) in 1,4-dioxane showed a red shift in emission by addition of methanol. This is due to the fact that the excited-state energy level of the dye decreases with an increase in the degree of aggregation because the PMMA matrix ($\varepsilon = 3.3$)[13] is more polar than 1,4-dioxane ($\varepsilon = 2.2$).[12] This result suggests that the fluorescence colors of the present copolymers can be precisely tuned by aggregation.

Another remarkable event is the change in fluorescence intensity by aggregation. Interestingly, the fluorescence of a nonpolar P(St-*co*-**2**) in polar DMF significantly decreased with an increase in the degree of aggregation, whereas that of a polar P(AN-*co*-**2**) in the polar DMF increased along with aggregation. This is explained in terms of oscillator strength (f)[14] of the polymers because the f indicates probability for electron transition from ground to excited state. The plots of f values as a function of the amount of added methanol are shown in Figure 5. The f values of P(St-*co*-**2**) significantly decrease with an increase in the degree of aggregation, while that of P(AN-*co*-**2**) increases. Accordingly, it should be said that the dye in nonpolar P(St-*co*-**2**) mainly undergoes a nonradiative process by aggregation while the dye in P(AN-*co*-**2**) aggregate prefers a direct, permitted transition to an indirect narrow band-gap transition.

Conclusion

We successfully synthesized a new pyran-based CTD monomer, **2**, by Knoevenagel reaction. Copolymerization of **2** with St, MMA, and AN afforded copolymers of P(St-*co*-**2**), P(MMA-*co*-**2**), and P(AN-*co*-**2**) with appropriate molecular weights. IR and UV−vis absorption study confirmed covalent incorporation of **2** into the copolymers. The **2** in the copolymers showed unusual photophysical properties which are completely different from **2**. All these copolymers showed blue shifts in emission relative to **2**. Also, their $\lambda_{\text{max,abs}}$ and $\lambda_{\text{max,em}}$ increased with an increase in dielectric constant of the polymer matrix. The copolymers in a polar solvent showed blue shifts in emission along with aggregation by addition of methanol while copolymers in a nonpolar solvent showed a red shift. The fluorescence intensity of P(St-*co*-**2**) and P(MMA-*co*-**2**) decreased by aggregation while that of P(AN-*co*-**2**) increased. We expect that such a solvatochromism and unusual aggregation behaviors are able to be subjected to an extended chemical selectivity in a volatile organic compound (VOC)-sensing performance. Thus, the present copolymers may be one of the promising candidates for a new VOC-sensing basic material.

Acknowledgment. This work was supported by the Korea Science and Engineering Foundation (KOSEF) grants funded by the Korea government (MEST) (R01-2008-000-10069-0, R11-2008-105-03002-0). This research was financially supported by the Minisitry of Education, Science Technology (MEST) and Korea Industrial Technology Foundation (KOTEF) through the Human Resource Training Project for Regional Innovation.

Supporting Information Available: ^{1}H NMR spectrum of **2** (Figure S1); UV−vis absorption spectra and calibration curve of absorbance of **2** (Figure S2); IR absorption spectra of P(St-*co*-**2**), P(MMA-*co*-**2**), and P(AN-*co*-**2**) (Figure S3). This material is available free of charge via the Internet at http://pubs.acs.org.

References and Notes

(1) (a) Webster, F. G.; McColgin, W. C. US Patent 3,852,683, Dec 3, 1974. (b) Hammond, P. R. *Opt. Commun.* **1979**, *29*, 331. (c) Antonov, V. S.; Hohla, K. L. *Appl. Phys.* **1983**, *B32*, 9. (d) Speiser, S.; Shakkour, N. *Appl. Phys.* **1985**, *B38*, 191. (e) Taylor, J. R. *Opt. Commun.* **1986**, *57*, 117.

(2) (a) de Silva, A. P.; Gunaratne, H. Q. N.; Gunnlaugsson, T.; Huxley, A. J. M.; McCoy, C. P.; Rademacher, J. T.; Rice, T. E. *Chem. Rev.* **1997**, *97*, 1515. (b) Suzuki, Y.; Yokoyama, K. *J. Am. Chem. Soc.* **2005**, *127*, 17799.

(3) (a) Batchelder, J. S.; Zewil, A. H.; Cole, T. *Appl. Opt.* **1981**, *20*, 3733. (b) Sansregret, J.; Drake, J. M.; Thomas, W. R. L.; Lesiecki, M. L. *Appl. Opt.* **1983**, *22*, 573.

(4) (a) Tang, C. W.; VanSlyke, S. A.; Chen, C. H. *J. Appl. Phys.* **1989**, *65*, 3610. (b) Bulovic, V.; Deshpande, R.; Thompson, M. E.; Forrest, S. R. *Chem. Phys. Lett.* **1999**, *308*, 317. (c) Zhang, X. H.; Chen, B. J.; Lin, X. Q.; Wong, Q. Y.; Lee, C. S.; Kwong, H. L.; Lee, S. T.; Wu, S. K. *Chem. Mater.* **2001**, *13*, 1565.

(5) See the related review papers: (a) Burland, D. M.; Miller, R. D.; Walsh, C. A. *Chem. Rev.* **1994**, *94*, 31. (b) Kanis, D. R.; Marks, T. J.; Ratner, M. A. *Chem. Rev.* **1994**, *94*, 195. (c) Long, N. J. *Angew. Chem., Int. Ed. Engl.* **1995**, *34*, 21. (d) Marks, T. J.; Ratner, M. A. *Angew. Chem., Int. Ed. Engl.* **1995**, *34*, 155. (f) Mishra, A.; Behera, R. K.; Behera, P. K.; Mishra, B. K.; Behera, G. B. *Chem. Rev.* **2000**, *100*, 1973. (g) Grabowski, Z. R.; Rotkiewicz, K.; Rettig, W. *Chem. Rev.* **2003**, *103*, 3899. (h) Zucchero, A. J.; Wilson, J. N.; Bunz, U. H. F. *J. Am. Chem. Soc.* **2006**, *128*, 11872–11881.

(6) See the related recent review paper: Kim, J.-M. *Macromol. Rapid Commun.* **2007**, *28*, 1191–1212, and references therein.

(7) (a) Uchiyama, S.; Matsumura, Y.; de Silva, A. P.; Iwai, K. *Anal. Chem.* **2003**, *75*, 5926–5935. (b) Uchiyama, S.; Matsumura, Y.; de Silva, A. P. *Anal. Chem.* **2004**, *76*, 1793–1798. (c) Uchiyama, S.; Kawai, N.; de Silva, A. P.; Iwai, K. *J. Am. Chem. Soc.* **2004**, *126*, 3032–3033. (d) Uchiyama, S.; McClean, G. D.; Iwai, K.; de Silva, A. P. *J. Am. Chem. Soc.* **2005**, *127*, 8920–8921. (e) Uchiyama, S.; Takehira, K.; Yoshihara, T.; Tobita, S.; Ohwada, T. *Org. Lett.* **2006**, *8*, 5869–5872. (f) Onoda, M.; Uchiyama, S.; Ohwada, T. *Macromolecules* **2007**, *40*, 9651–9657.

(8) (a) Zhu, M.-Q.; Zhu, L.; Han, J. J.; Wu, W.; Hurst, J. K.; Li, A. D. Q. *J. Am. Chem. Soc.* **2006**, *128*, 4303–4309. (b) Zhang, G.; Chen, J.; Payne, S. J.; Kooi, S. E.; Demas, J. N.; Fraser, C. *J. Am. Chem. Soc.* **2007**, *129*, 8942–8943.

(9) (a) Alam, M. M.; Jenekhe, S. A. *Chem. Mater.* **2002**, *14*, 4775–4780. (b) Ego, C.; Marsitzky, D.; Becker, S.; Zhang, J.; Grimsdale, A. C.; Mullen, K.; Mackenzie, J. D.; Silva, C.; Friend, R. H. *J. Am. Chem. Soc.* **2003**, *125*, 437–443. (c) Mochizuki, H.; Hasui, T.; Kawamoto, M.; Ikeda, T.; Adachi, C.; Taniguchi, Y.; Shirota, Y. *Macromolecules* **2003**, *36*, 3457–3464. (d) Cheon, C. H.; Joo, S.-H.; Kim, K.; Jin, J.-I.; Shin, H.-W.; Kim, Y.-R. *Macromolecules* **2005**, *38*, 6336–6345. (e) Nielson, K. T.; Spanggaard, H.; Krebs, F. C. *Macromolecules* **2005**, *38*, 1180–1189. (f) Su, H.-J.; Wu, F.-I.; Shu, C.-F. *Macromolecules* **2004**, *37*, 7197–7202. (g) Wu, F.-I.; Shih, P.-I.; Shu, C.-F.; Tung, Y.-L.; Chi, Y. *Macromolecules* **2005**, *38*, 9028–9036. (h) Zhen, H.; Luo, C.; Yang, W.; Song, W.; Du, B.; Jiang, J.; Jiang, C.; Zhang, Y.; Cao, Y. *Macromolecules* **2006**, *39*, 1693–1700. (i) Chuang, C.-Y.; Shih, P.-I.; Chien, C.-H.; Wu, F.-I.; Shu, C.-F. *Macromolecules* **2007**, *40*, 247–252. (j) Gomez, R.; Veldman, D.; Blanco, R.; Seoane, C.; Segura, J. L.; Janssen, R. A. J. *Macromolecules* **2007**, *40*, 2760–2772.

(10) (a) Deans, R.; Kim, J.; Machacek, M. R.; Swager, T. M. *J. Am. Chem. Soc.* **2000**, *122*, 8565–8566. (b) Luo, J.; Lam, Xie, Z. J. W. Y.; Cheng, L.; Chen, H.; Qiu, C.; Kwok, H. S.; Zhang, X.; Zhan, X.; Liu, Y.; Zhu, D.; Tang, B. Z. *Chem. Commun.* **2001**, 1740–1741. (c) Levitus, M.; Schmieder, K.; Ricks, H.; Shimizu, K. D.; Bunz, U. H. F.; Garcia-Garibay, M. A. *J. Am. Chem. Soc.* **2001**, *123*, 4259–4265. (d) An, B.-K.; Kwon, S.-K.; Jung, S.-D.; Park, S. Y. *J. Am. Chem. Soc.* **2002**, *124*, 14410–14415. (e) Xiao, D.; Xi, L.; Yang, W.; Fu, H.; Shuai, Z.; Fang, Y.; Yao, J. *J. Am. Chem. Soc.* **2003**, *125*, 6740–6745. (f) An, B.-K.; Lee, D.-S.; Lee, J.-S.; Park, Y.-S.; Song, H.-S.; Park, S. Y. *J. Am. Chem. Soc.* **2004**, *126*, 10232–10233. (g) Wang, F.; Han, M.-Y.; Myya, K. Y.; Wang, Y.; Lai, Y.-H. *J. Am. Chem. Soc.* **2005**, *127*, 10350–10355. (h) Dong, Y.; Lam, J. W. Y.; Qin, A.; Sun, J.; Liu, J.; Li, Z.; Sun, J.; Sung, H. H. Y.; Williams, I. D.; Kwok, H. S.; Tang, B. Z. *Chem. Commun.* **2007**, 3255–3257. (i) Qian, Y.; Li, S.; Zhang, G.; Wang, Q.; Wang, S.; Xu, H.; Li, C.; Li, Y.; Yang, G. *J. Phys. Chem. B* **2007**, *111*, 5861–5868. (j) Wang, Y.; Park, J. S.; Leech, J. P.; Miao, S.; Bunz, U. H. F. *Macromolecules* **2007**, *40*, 1843–1850. (k) Cardolaccia, T.; Li, Y.; Schanze, K. S. *J. Am. Chem. Soc.* **2008**, *130*, 2535–2545.

(11) Kwak, G.; Wang, S.; Choi, M.-S.; Kim, H.; Choi, K.-H.; Han, Y.-S.; Hur, Y.; Kim, S.-H. *Dyes Pigments* **2008**, *78*, 25–33.

(12) (a) Mark, J. E. *Polymer Data Handbook*; Oxford University Press: New York, 1999. (b) Lide, D. R. *Handbook of Organic Solvent*; CRC Press: Boca Raton, FL, 1994.

(13) Kwak, G.; Okada, C.; Fujiki, M.; Takeda, H.; Nishida, T.; Shiosaki, T. *Jpn. J. Appl. Phys.* **2008**, *47*, 1753–1756.

(14) (a) Barrow, G. M. *Physical Chemistry*, 6th ed.; McGraw-Hill: New York, 1996. (b) Silbey, R. J. *Physical Chemistry*, 4th ed.; Wiley: Hoboken, NJ, 2005.

MA802532B